Bonding Analysis in Inorganic Transition-Metal Cubic Clusters. 1. Noncentered Hexacapped $M_8(\mu_4\text{-}E)_6L_n$ ($n \leq 8$) Species

Eric Furet, Albert Le Beuze, Jean-François Halet,* and Jean-Yves Saillard*

Contribution from the Laboratoire de Chimie du Solide et Inorganique Moléculaire, URA CNRS 1495, Université de Rennes I, 35042 Rennes Cedex, France

Received August 5, 1993. Revised Manuscript Received October 4, 1993®

Abstract: The bonding in cubic $M_8(\mu_4\text{-}E)_6L_n$ cluster compounds is analyzed by means of extended Hückel and self-consistent field multiple-scattering $X\alpha$ calculations. The results indicate that an optimal number of metallic valence electrons (MVEs) of 120 is favored with electronegative metals and/or terminal π-acceptor ligands. The rather strong M–M bonding is mainly due to through-space M–M interactions but also to through-bond M–E interactions. A delocalized bonding picture is therefore necessary to describe the electronic structure of these species. For the 120-electron count, the M–(μ_4-E) bonding is maximized, whereas the M–M bonding is not. The latter is strengthened upon depopulation of the top of the d band. Open-shell electronic configurations are then expected for clusters bearing terminal π-donor ligands. The slight antibonding/nonbonding nature of the top of the metallic d band allows a large range of electron counts (from 99 to 120 so far) without altering the cubic metallic core. When terminal ligands borne by the metal atoms are missing, the favored count for compounds of formula $M_8(\mu_4\text{-}E)_6L_n$ is $120 - 2(8 - n)$ MVEs. M–L bonds result primarily from the combination of a metallic sp hybrid and the σ lone pair orbital of L. When n terminal ligands are lost, the n corresponding metallic hybrids become nonbonding but remain high in energy and are vacant, leading to an electron count diminished by $2n$ units compared to that of the $M_8(\mu_4\text{-}E)_6L_8$ parent species.

Introduction

Since Lower and Dahl first prepared $Ni_8(\mu_4\text{-}PPh)_6(CO)_8$ (**1**, Chart 1),[1] several cubic transition-metal complexes have been characterized with the impetus of leading groups as those of Fenske,[2–8] Holm,[9] or Pohl.[10–12] Table 1 summarizes some relevant data for hexacapped cubic clusters of formula $M_8(\mu_4\text{-}E)_6L_n$ (M = transition metal, E = main group element, L = two-electron terminal ligand (CO, PR_3, Cl^-, ...), and $n \leq 8$) which have been characterized by X-ray diffraction.

These compounds belong to the family of capped three-connected polyhedral clusters which are generally characterized by $3n$ skeletal electrons (n represents the number of metallic centers of the cluster cage) or $15n$ metallic valence electrons (MVEs).[13] The count of 24 skeletal electrons or 120 MVEs for **1** [10(Ni)(8) + 2(CO)(8) + 4(PPh)(6) = 15(8) = 120) is then in agreement with these electron-counting rules. However, this is not the case for a large number of the compounds listed in Table 1. The valence electron count can vary importantly, from 99 to 120, for the same relatively regular cubic architectural unit. There is, however, some shortening of the metal–metal separation with the diminution of the electron count. For instance, the averaged Ni–Ni distance is 2.53 Å in the 112-MVE $Ni_8(\mu_4\text{-}PPh)_6(PPh_3)_4$ compound (**19**),[4,8] versus 2.67 Å in the 120-MVE $Ni_8(\mu_4\text{-}PPh)_6(PPh_3)_4(CO)_4$ species (**2**).[2] The first question which arises then is the following: how many electrons are responsible for the metal–metal bonds in these species, in which the observed M–M bond distances are comparable to those measured in the corresponding metallic elements?[14] In contrast, for a given electron count the nature of the capping ligands seems at first sight to play a minor role in the M–M separations. One should mention that the capping units encountered in these cubic complexes are isolobal[15] and have similar sizes.

Chart 1

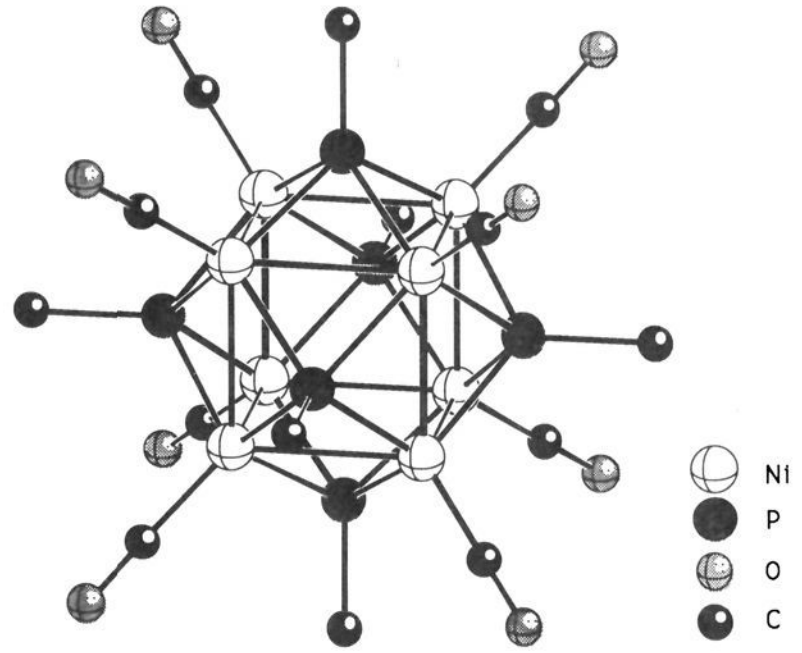

® Abstract published in *Advance ACS Abstracts,* December 1, 1993.

(1) Lower, L. D.; Dahl, L. F. *J. Am. Chem. Soc.* **1976**, *98*, 5046.
(2) Fenske, D.; Basoglu, R.; Hachgenei, J.; Rogel, F. *Angew. Chem., Int. Ed. Engl.* **1984**, *23*, 160.
(3) Fenske, D., personal communication.
(4) Fenske, D.; Magull, J. *Z. Naturforsch.* **1990**, *45b*, 121.
(5) Fenske, D.; Krautscheid, H.; Müller, M.-H. *Angew. Chem., Int. Ed. Engl.* **1992**, *31*, 321.
(6) Fenske, D.; Hachgenei, J.; Ohmer, J. *Angew. Chem., Int. Ed. Engl.* **1985**, *24*, 706.
(7) Fenske, D.; Ohmer, J.; Hachgenei, J.; Merzweiler, K. *Angew. Chem., Int. Ed. Engl.* **1988**, *27*, 1277.
(8) Fenske, D.; Hachgenei, J.; Rogel, F. *Angew. Chem., Int. Ed. Engl.* **1984**, *23*, 982.
(9) Christou, G.; Hagen, K. S.; Bashkin, J. K.; Holm, R. H. *Inorg. Chem.* **1985**, *24*, 1010.
(10) (a) Pohl, S.; Opitz, U. *Angew. Chem., Int. Ed. Engl.* **1993**, *32*, 863. (b) Pohl, S.; Barklage, W.; Saak, W.; Opitz, U. *J. Chem. Soc., Chem. Commun.* **1993**, 1251.
(11) Pohl, S.; Saak, W. *Angew. Chem., Int. Ed. Engl.* **1984**, *23*, 907.
(12) Saak, W.; Pohl, S. *Angew. Chem., Int. Ed. Engl.* **1991**, *30*, 881.
(13) Johnston, R. L.; Mingos, D. M. P. *J. Organomet. Chem.* **1985**, *280*, 407.
(14) Greenwood, N. N.; Earnshaw, A. *Chemistry of the Elements*; Pergamon Press, Inc.: New York, 1984; pp 1248, 1294, 1333.
(15) (a) Hoffmann, R. *Angew. Chem., Int. Ed. Engl.* **1982**, *21*, 711. (b) Evans, D. G.; Mingos, D. M. P. *J. Organomet. Chem.* **1985**, *295*, 389.

0002-7863/94/1516-0274$04.50/0

Table 1. Molecular Cubic $M_8(\mu_4\text{-}E)_6L_n$ Clusters Characterized by X-ray Diffraction

compound	$d_{M\text{-}M}$[a]	MVE[b]	remarks	ref
(a) $M_8(\mu_4\text{-}E)_6L_8$				
$Ni_8(\mu_4\text{-}PPh)_6(CO)_8$ (**1**)	2.65	120	diam[c] black	1
$Ni_8(\mu_4\text{-}PPh)_6(PPh_3)_4(CO)_4$ (**2**)	2.67	120	diam	2
$Ni_8(\mu_4\text{-}PPh)_6(CO)_4(AsPh_3)_4$ (**3**)		120		3
$Ni_8(\mu_4\text{-}S)_6(PPh_3)_8$ (**4**)	2.70	120		4
$Ni_8(\mu_4\text{-}Se)_6(Pn\text{-}Bu_3)_8$ (**5**)	2.70	120		5
$Ni_8(\mu_4\text{-}S)_6(PPh_3)_6Cl_2$ (**6**)	2.68	118	dist[d]	6
$Ni_8(\mu_4\text{-}PPh)_6(PPh_3)_4Cl_4$ (**7**)	2.61	116	param[c]	2
$Ni_8(\mu_4\text{-}PPh)_6(PPh_3)_4Br_4$ (**8**)	2.61	116	param	2
$[Ni_8(\mu_4\text{-}PPh)_6(PPh_3)_4Cl_4]^+$ (**9**)	2.58	115	param	7
$[Co_8(\mu_4\text{-}S)_6(SPh)_8]^{4-}$ (**10**)	2.66	108	black	9
$[Co_8(\mu_4\text{-}S)_6(SPh)_8]^{5-}$ (**11**)	2.67	109	black	9
$[Fe_8(\mu_4\text{-}S)_6I_8]^{4-}$ (**12**)	2.72	100	black	10
$[Fe_8(\mu_4\text{-}S)_6I_8]^{3-}$ (**13**)	2.72	99	black	11
$Ni_5Fe_3(\mu_4\text{-}S)_6I_8^{4-}$ (**14**)	2.68	110		12
(b) $M_8(\mu_4\text{-}E)_6L_n$ ($n < 8$)				
$Ni_8(\mu_4\text{-}Se)_6(PEt_2Ph)_6$ (**15**)		116	dist, black	5
$Ni_8(\mu_4\text{-}PPh)_6(PPh_3)_4Ni$ (**16**)	2.54	114	param, dist	8
$Ni_8(\mu_4\text{-}PPh)_6(PPh_3)_4Hg$ (**17**)	2.53	114		4
$Ni_8(\mu_4\text{-}Se)_6(Pi\text{-}Pr_3)_4$ (**18**)		112	dist, black	5
$Ni_8(\mu_4\text{-}PPh)_6(PPh_3)_4$ (**19**)	2.53	112	param, dist	4, 8

[a] Averaged metal–metal distance (Å). [b] Total valence metallic electron count. [c] diam, diamagnetic; param, paramagnetic. [d] dist, distorted.

The clusters listed in Table 1 can be divided in two groups. The first one is made of compounds bearing a terminal ligand on each metallic atom ($n = 8$). This set itself can be separated in two categories: those having 120 MVEs and bearing 8 more or less π-acceptor terminal ligands (CO, PR_3) and those, poorer in electrons, possessing some π-donor ligands (Cl, Br). Compounds presenting an incomplete shell of terminal ligands ($n < 8$) constitute the second group. They always possess fewer than 120 MVEs.

Similar cubic architectures are also encountered in solid-state chemistry, such as in natural ((Fe, Co, or Ni)$_9S_8$)[16] and synthetic (Co_9S_8)[17] pentlandites and in djerfisherites such as $K_6LiFe_{24}S_{26}Cl$[18] or $Ba_6Co_{25}S_{27}$.[19] Metallic behavior is usually observed in these compounds presenting $M_8(\mu_4\text{-}S)_6$ entities, which often formally possess 112 MVEs.

Several theoretical studies have been done on some of the compounds given in Table 1. Some years ago, Burdett and Miller studied the bonding in the solid-state pentlandite structures and their molecular analogous from extended Hückel (EH) results.[20] Hoffman, Bashkin, and Karplus have used EH and self-consistent field multiple-scattering Xα (Xα) calculations to examine the electronic structures of molecular cubic clusters containing a Co_9S_8 core.[21] Very recently Rösch, Ackermann, and Pacchioni have performed some linear combination of Gaussian-type orbitals local density functional (LCGTO-LDF) calculations in order to analyze the metal–metal bonding in $Ni_8(\mu_4\text{-}PPh)_6(CO)_8$.[22] To date, however, no complete study has been done on the whole set of clusters listed in Table 1. This paper presents a detailed rationalization of the bonding in these compounds and the properties associated with their electron count, based on EH and Xα calculations. The computational details are gathered in the Appendix.

Electronic Structure of the 120-Electron Cubic Species $M_8(\mu_4\text{-}E)_6L_8$

(a) Qualitative Approach. The electronic structure of the 120-electron cubic species $Ni_8(\mu_4\text{-}E)_6L_8$ (E = S, Se, PR; L = CO, PR_3, AsR_3)[1-5] (**1–5**) is often described in terms of a localized bonding scheme, i.e., represented by a Lewis structure with 2-center/2-electron bonds, in which the M–M bonding is considered as "cubane-like".[13] Within such a bonding model, the transition-metal atoms obey the 18-electron rule, but the main-group E atoms, being pentavalent, do not follow the octet rule. However, localized Lewis formulae are inadequate in describing properly the bonding in hypervalent molecules.[23] Indeed, each capping main-group atom or group of atoms like PR possesses only three frontier molecular orbitals (FMO) to ensure the bonding with the metallic square to which it is tethered (see the right-hand side of Figure 1). It follows that only a delocalized MO description of the 120-electron species **1–5** can account for the nature ("cubane-like" or not) of the M–M bonding. This can be done by deriving the MO diagram of the 120-electron species $Ni_8(\mu_4\text{-}E)_6L_8$ with O_h symmetry from the interaction of a $[Ni_8L_8]^{12+}$ cube with a capping $[E_6]^{12-}$ octahedron. The FMOs of the $[Ni_8L_8]^{12+}$ entity can qualitatively be obtained by combining the FMOs of the eight Ni–L fragments. Such a fragment, as shown on the left-hand side of Figure 1, presents a block of five d-type orbitals (one, two, and two of σ, π, and δ symmetry, respectively). Above lie a radial σ-type sp hybrid and a set of two tangential π-type orbitals of Ni 4p parentage.[15]

One can deduce from group theory that the three upper FMOs (sp_σ and p_π) of the Ni–L units generate a set of 12 bonding MOs ($a_{1g} + e_g + t_{2g} + t_{1u} + t_{2u}$), largely separated from a set of 12 antibonding MOs ($t_{1g} + t_{2g} + a_{2u} + e_u + t_{1u}$), which is expected to lie at very high energy. Similarly, the combination of the three lower d_σ and d_π orbitals leads to the formation of a set of bonding ($a_{1g} + e_g + t_{2g} + t_{1u} + t_{2u}$) and a set of antibonding ($t_{1g} + t_{2g} + a_{2u} + e_u + t_{1u}$) levels. However, because d-type FMOs of the M–L fragments are more contracted than the s- and p-type ones, they overlap less strongly in the cube. Consequently, the energy separation between the two sets of combinations is expected to be smaller. The two δ-type FMOs are expected to interact weakly, giving rise to a block of MOs more or less nonbonding ($e_g + t_{1g} + t_{2g} + e_u + t_{1u} + t_{2u}$). They should be found intercalated between the bonding and antibonding sets descending from the d_σ and d_π FMOs. The resulting level ordering for the $[Ni_8L_8]^{12+}$ moiety is given on the left-hand side of Figure 1. Of course, second-order interactions between combinations of the same symmetry are expected to occur. This must lead to some $\sigma/\pi/\delta$ mixing and particularly to some hybridization of the d block, giving rise to a significant enhancement of the bonding character of the 12 lowest levels and a lowering of the antibonding character of the 12 antibonding counterparts.[22] However, it is not expected to perturb much the general energy order.

The three FMOs of the six noninteracting E groups constituting the octahedral $[E_6]^{12-}$ moiety combine with each other to give a set of 18 nonbonding MOs, 6 of σ-type ($a_{1g} + e_g + t_{1u}$) and 12 of π-type ($t_{1g} + t_{2g} + t_{1u} + t_{2u}$). This block of levels is represented on the right-hand side of Figure 1.

The major bonding interactions (i.e., 2-electron/2-orbital) between the two fragments $[Ni_8L_8]^{12+}$ and $[E_6]^{12-}$ are expected to occur between the 18 occupied FMOs associated with $[E_6]^{12-}$ and the 18 lowest unoccupied FMOs of $[Ni_8L_8]^{12+}$ of the same symmetry. Among these vacant FMOs, only 6 can come from the upper part of the d block (the 34 remaining ones are occupied, see above), while 12 come from the Ni–Ni s + p bonding block ($a_{1g} + e_g + t_{2g} + t_{1u} + t_{2u}$). It follows that the six d-type metallic

(16) (a) Vaughan, D. J.; Craig, J. R. *Mineral Chemistry of Metal Sulfides*; Cambridge University Press: New York, 1978. (b) Rajamani, V.; Prewitt, C. T. *Can. Mineral.* **1973**, *12*, 178; *Am. Mineral.* **1975**, *60*, 39.
(17) (a) Rajamani, V.; Prewitt, C. T. *Can. Mineral.* **1975**, *13*, 75. (b) Kim, K.; Dwight, K.; Wold, A.; Chianelli, R. R. *Mater. Res. Bull.* **1981**, *16*, 1319. (c) Pasquariello, D. M.; Kershaw, R.; Passaretti, J. D.; Dwight, K.; Wold, A. *Inorg. Chem.* **1984**, *23*, 872.
(18) (a) Tani, B. S. *Am. Mineral.* **1977**, *62*, 819. (b) Czamanske, G. K.; Erd, R. C. *Am. Mineral.* 1979, *64*, 776.
(19) Snyder, G. J.; Badding, M. E.; DiSalvo, F. J. *Inorg. Chem.* **1992**, *31*, 2107.
(20) Burdett, J. K.; Miller, G. J. *J. Am. Chem. Soc.* **1987**, *109*, 4081.
(21) Hoffman, G. G.; Bashkin, J. K.; Karplus, M. *J. Am. Chem. Soc.* **1990**, *112*, 8705.
(22) Rösch, N.; Ackermann, L.; Pacchioni, G. *Inorg. Chem.* **1993**, *32*, 2963.
(23) Albright, T. A.; Burdett, J. K.; Whangbo, M. H. *Orbital Interactions in Chemistry*; John Wiley & Sons, Inc.: New York, 1985; p 258.

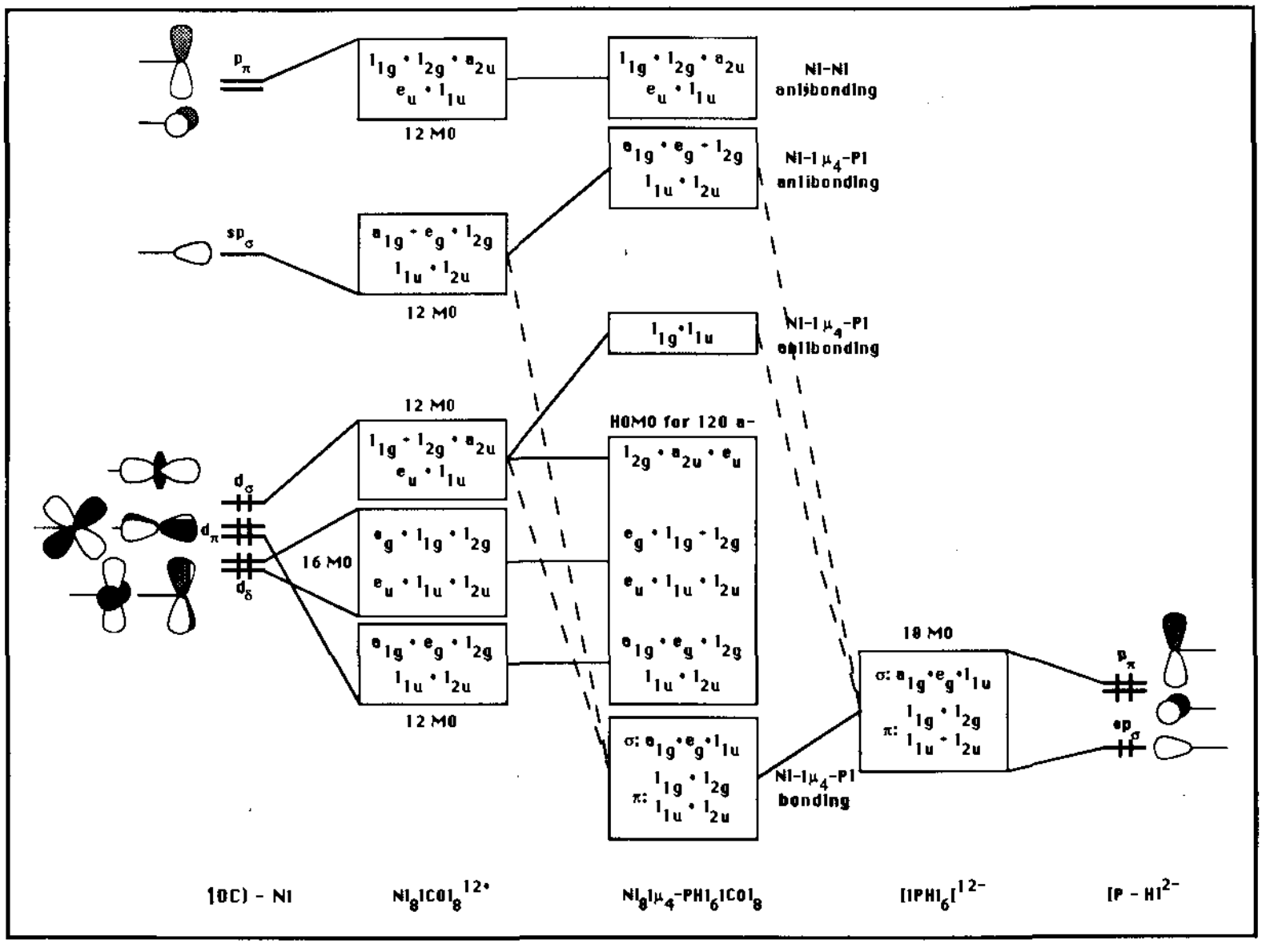

Figure 1. Qualitative MO diagram for the model $Ni_8(\mu_4\text{-}PH)_6(CO)_8$ obtained from the interaction of the cubic $[Ni_8(CO)_8]^{12+}$ and octahedral $[(PH)_6]^{12-}$ fragments. The FMOs of the Ni(CO) and PH moieties are shown on the far left- and far right-hand sides, respectively.

orbitals involved in the interaction are necessarily of t_{1g} and t_{1u} symmetry. The resulting qualitative diagram of a 120-electron $[Ni_8(\mu_4\text{-}E)_6L_8]$ species is illustrated in the middle of Figure 1. The Ni–Ni bonding is expected to be enhanced by some participation of high-lying (s + p) Ni–Ni bonding FMOs in occupied levels. However, the main Ni–Ni bonding might come, as we shall see later, from the lower metallic d set ($a_{1g} + e_g + t_{2g} + t_{1u} + t_{2u}$), which could be then associated with the 12 Ni–Ni bonds. Obviously, the simplified diagram of Figure 1, which does not take into account 4-electron/2-orbital destabilizations and second-order mixing, cannot be used to predict the level ordering inside the occupied d block. However, it provides a general understanding of the chemical bonding in the clusters considered.

(b) EH and Xα Calculations on $Ni_8(\mu_4\text{-}PH)_6(CO)_8$. The MO diagrams of the d block obtained from the EH and Xα methods on the cluster model $Ni_8(\mu_4\text{-}PH)_6(CO)_8$ are given on the left- and right-hand sides of Figure 2, respectively. The values given in brackets correspond to the percentage metallic character. It is noteworthy that both types of calculations are in close agreement, leading to similar electronic configuration, level ordering, and energy gaps. They are also in qualitative agreement with the simplified diagram described in Figure 1. This similarity between the EH and Xα results brings some confidence in the use of the extended Hückel method on this kind of cluster compounds. The six vacant d levels ($3t_{1u}$, $2t_{1g}$) are well separated from the rest of the d block, which is occupied. A significant HOMO ($3t_{2g}$)/LUMO ($2t_{1g}$) gap is computed. As already mentioned by Burdett and Miller,[20] the HOMO appears energetically isolated, lying about 1 eV above the next group of occupied levels ($2t_{1u} + 2e_g + 1a_{2u}$).

Figure 3 shows the nickel–nickel (left) and nickel–phosphorus (right) overlap populations plotted with respect to the energy obtained from our EH calculations. As anticipated previously, only the vacant $3t_{1u}$ and $2t_{1g}$ levels are both strongly Ni–Ni and

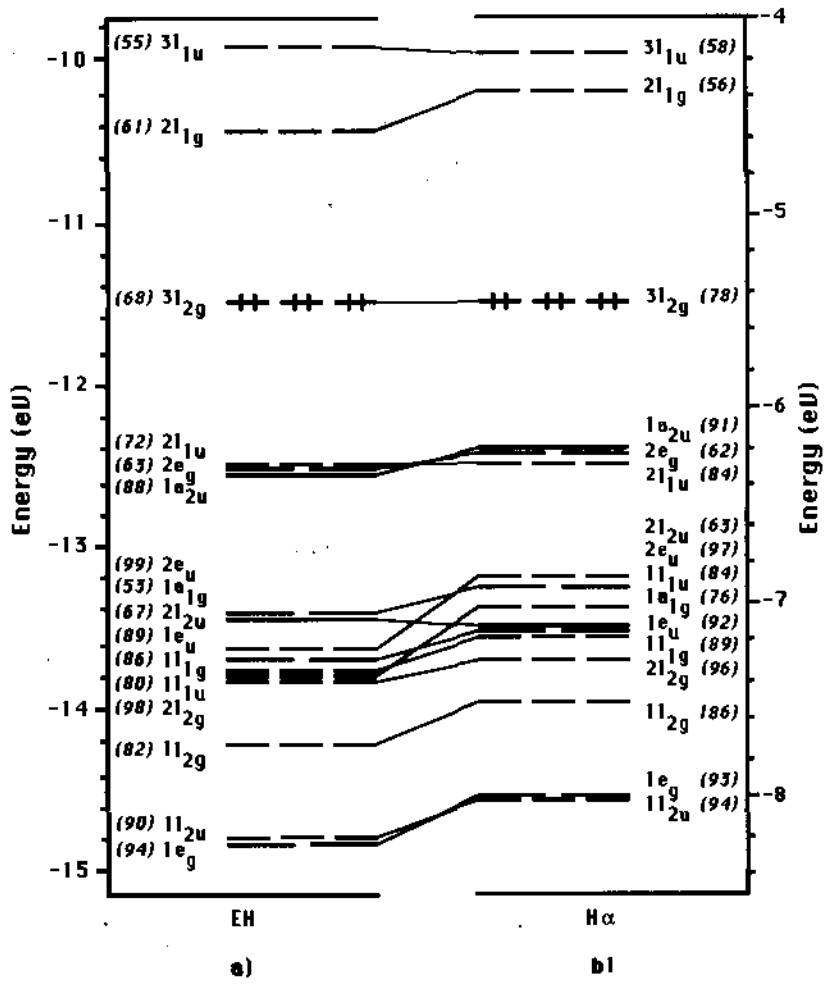

Figure 2. Molecular orbital d block for the model $Ni_8(\mu_4\text{-}PH)_6(CO)_8$ obtained from EH (a) and Xα (b) calculations. Numbers in brackets indicate the percentage metallic character.

Ni–P antibonding. The computed Ni–Ni overlap population is 0.06 for a count of 120 MVEs. The major part of this bonding comes from the occupied d block. As predicted from Figure 1, some occupied metallic levels such as $3t_{2g}$, $1a_{2u}$, and $2e_u$ are somewhat Ni–Ni antibonding. Therefore, in these 120-electron

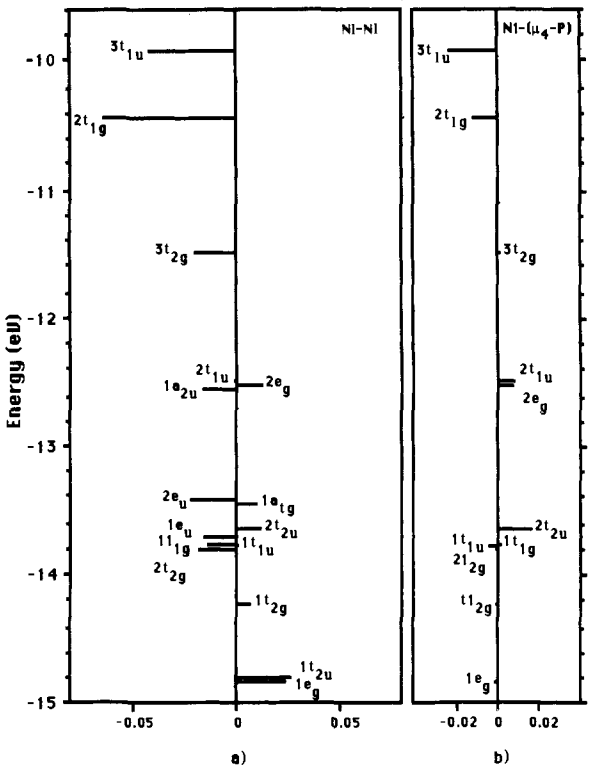

Figure 3. Ni–Ni (a) and Ni–(μ_4-P) (b) molecular orbital overlap populations in $Ni_8(\mu_4\text{-}PH)_6(CO)_8$, obtained from EH calculations.

cubic species, the Ni–Ni bonding is not maximized. On the other hand, for the same electron count, the Ni–P bonding interaction is maximized (corresponding overlap population 0.48). This suggests that the electron count of these cubic M_8E_6 compounds is primarily governed by the M–E rather than by the M–M interactions.[20]

We would like to end the discussion on the 120-electron species $Ni_8(\mu_4\text{-}E)_6L_8$ by coming back to its comparison with cubane, C_8H_8.[24] The skeletal MOs of cubane are easily derived from the interaction of the FMOs of the eight (CH) units.[25] Among the 24 combinations, 12 are occupied and more or less bonding ($a_{1g} + e_g + t_{2g} + t_{1u} + t_{2u}$), while 12 are vacant and antibonding ($t_{1g} + t_{2g} + a_{2u} + e_u + t_{1u}$). Although the 120-electron cubic species $Ni_8(\mu_4\text{-}PH)_6(CO)_8$ follows the electron counting rule for the three-connected transition-metal clusters ($15n$),[13] its electronic structure differs somewhat from that of cubane. It is possible to extract a set of 12 Ni–Ni bonding MOs from the bottom of the d block having the same nodal characteristics as those of the 12 bonding MOs of cubane ($1e_g$, $1t_{2u}$, $1t_{2g}$, $1t_{1u}$, and $1a_{1g}$ in Figure 2). These MOs are responsible for the major part of the Ni–Ni bonding, but because of second-order mixing, other metallic MOs such as $2t_{2u}$ or $2e_g$ are also Ni–Ni bonding. In addition, some Ni–Ni bonding character is also contained in the 18 occupied Ni–P MOs (see the Qualitative Approach section). More importantly and despite the second-order mixing with the Ni–Ni s + p bonding block, occupied d levels of the $t_{2g} + a_{2u} + e_u$ symmetry present some antibonding character (see Figures 1 and 2). Therefore, if as in the case of cubane, it is possible to identify 12 Ni–Ni bonding pairs in the 120-electron compound $Ni_8(\mu_4\text{-}PH)_6(CO)_8$, the somewhat antibonding nature of some occupied d levels does not allow a full analogy between the two compounds.

Fewer Electrons: The Electronic Structure of the Electron-Deficient $M_8(\mu_4\text{-}E)_6L_8$ Species

A localized M–M bonding scheme completely analogous to the C–C one in cubane would be reached if only 12 strongly M–M bonding levels of $a_{1g} + t_{1u} + e_g + t_{2u} + t_{2g}$ symmetry belonging to the d block were occupied. This hypothetical situation, which would correspond to a count of 76 MVEs, could be envisaged with early transition metals rather poor in electrons and possessing diffuse atomic orbitals. Formulae such as $Nb_8(\mu_4\text{-}PR)_6(PR'_3)_8$ or $[Mo_8(\mu_4\text{-}GeR)_6Cl_8]^{2-}$ could then be suggested.

The actual electron counts for the cubic $M_8E_6L_8$ species range from 99 to 120 (see Table 1). It appears that the 120-electron count observed for some nickel compounds is the maximum which can be encountered. Additional electrons would be housed in the $2t_{1g}$ and $3t_{1u}$ levels, which are strongly M–M and M–E antibonding (see Figure 3), and consequently would lead to some destabilizing effect for such a structural arrangement. On the other hand, the removal of electrons seems more favorable. Most of the levels near the $3t_{2g}$ HOMO are delocalized over the whole cube and weakly M–M antibonding ($3t_{2g}$, $2t_{1u}$, $1a_{2u}$) or bonding ($2e_g$). This relatively weak character is confirmed by their slight energy change upon the M–M bond length variation, as shown by our EH calculations. Their depopulation might then be possible, leading either to a very weak Jahn–Teller instability or to high-spin configurations, which would hardly alter the metallic cubic arrangement. These conclusions are in accord with the compounds listed in Table 1. Their M_8E_6 core is close to O_h symmetry whatever their electron count is, and some electron-deficient species are paramagnetic according to experimental work.[2,7] The moderate M–M antibonding character noted for some MOs which might be depopulated is confirmed by the weak diminution of the Ni–Ni separations in the electron-deficient nickel species compared to that of the 120-electron ones (see Table 1).

According to Table 1, the total electron count for the $M_8(\mu_4\text{-}E)_6L_8$ compounds varies with the nature of the metal centers and the σ- or π-donor capabilities of the terminal ligands but not with the nature of the capping E atoms. EH calculations were carried out on different cluster models, $Ni_8(\mu_4\text{-}PH)_6L_8$ (O_h) and $Ni_8(\mu_4\text{-}PH)_6L_4L'_4$ (T_d), with L, L' = CO, PH_3, or Cl^-. Their d-block MO diagram is shown in Figure 4. The replacement of the strong π-acceptor CO ligands by weak π-acceptor phosphines hardly perturbs the electronic structure of the metallic cubic core. A rather important HOMO–LUMO gap is preserved for the count of 120 MVEs, in agreement with the characterized cubic clusters bearing phosphine (or arsine) ligands. Despite the fact that a HOMO–LUMO gap is also computed in $Ni_8(\mu_4\text{-}PH)_8Cl_8$ for the count of 120 electrons, the substitution of the carbonyls by π-donor chlorines modifies somewhat the nature and the energy of some levels of the metallic d block. Some MOs which were slightly Ni–CO bonding are now destabilized, being Ni–Cl antibonding. This is particularly the case for the $2e_g$ level, which joins the $3t_{2g}$ orbital in $Ni_8(\mu_4\text{-}PH)_8L_8$ (HOMO for the 120-MVE count). An analogous destabilization, but less pronounced, is observed when only four chlorine ligands are present (see Figure 4). From these results and the analysis of Table 1, one can deduce that compounds of the general formula $M_8(\mu_4\text{-}PR)_6L_{8-n}L'_n$ (L = π-acceptor; L' = π-donor; $0 \le n \le 8$) are characterized by $110 \le MVE \le 120$. This electron count should correspond to the ($2e_g + 3t_{2g}$) MO set being totally filled, partly filled, or empty. The observed electron count seems to be roughly related to the number of π-donor ligands according to the rule MVE = 120 – n.

When the capping phosphido groups are replaced by chalcogenide atoms, low-lying σ(P–R) bonding doublets are replaced by high-lying lone pairs. In the O_h symmetry these lone pairs give rise to the ($a_{1g} + e_g + t_{1u}$) combinations. Their presence on the cluster leads to some destabilization of the d-block levels having the same symmetry, favoring MVE counts lower than 120. When π-donor terminal ligands are also present, low electron counts are particularly favored (see compounds **10–14** in Table 1). In that case, the $2e_g$ level lies above the $3t_{2g}$ one. These results are in general agreement with the previous studies of Burdett and Miller[20] and Hoffman, Bashkin, and Karplus.[21]

Pohl and collaborators have recently characterized cubic iron compounds of formulae $[Fe_8(\mu_4\text{-}S)_6I_8]^{4-}$ (**12**)[10a] and $[Fe_8(\mu_4$-

(24) (a) Eaton, P. E.; Cole, T. W. *J. Am. Chem. Soc.* **1964**, *86*, 3157. (b) Fleischer, E. B. *Ibid.* **1964**, *86*, 3889.
(25) Schulman, J. M.; Fischer, C. R.; Solomon, P.; Venanzi, T. J. *J. Am. Chem. Soc.* **1978**, *100*, 2949.

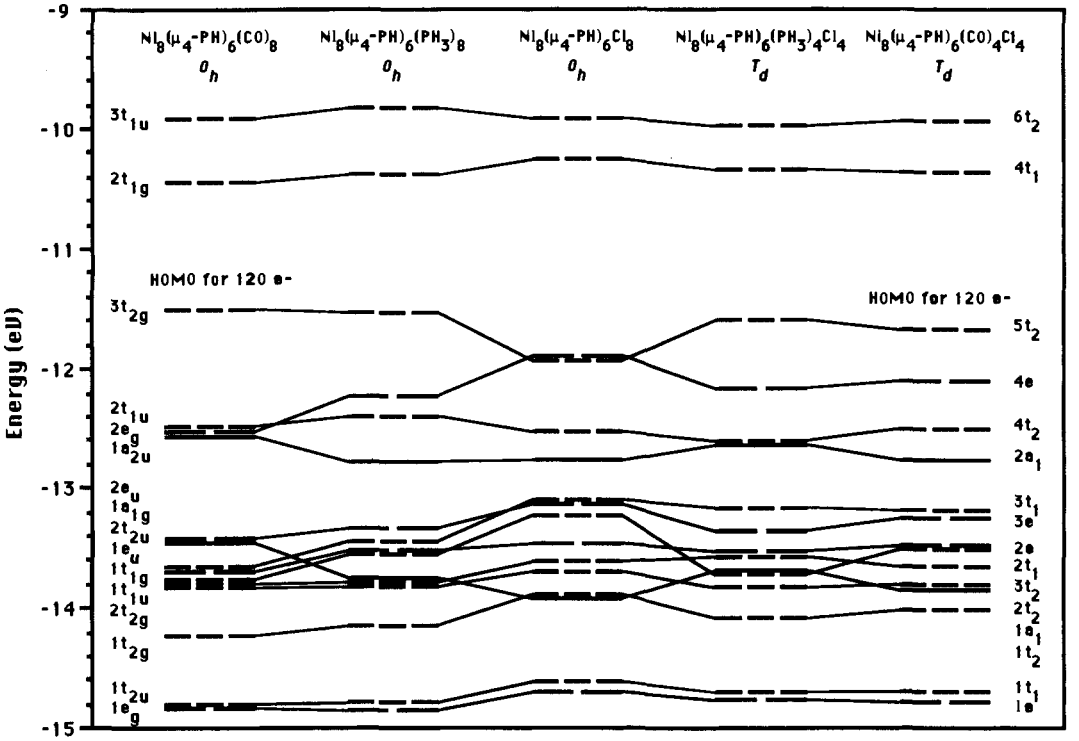

Figure 4. EH MO correlation diagram for the d block in several models $Ni_8(\mu_4\text{-}PH)_6L_4L'_4$ (L, L' = CO, PH_3, or Cl).

$S)_6I_8]^{3-}$ (**13**),[11] which may serve as models for active centers of iron–sulfur proteins.[26] A $[Fe_8(\mu_4\text{-}S)_6I_8]^{4-}$ core is also contained in the novel cluster $(MeCN)_8(Ph_2MePS)_2Ru_2Fe_8S_6I_8$.[10b] So far, the 100- and 99-electron counts of **12** and **13**, respectively, are the lowest observed for cubic M_8E_6 compounds (see Table 1). We have undertaken EH and Xα calculations on these species with an idealized O_h symmetry in order to get some informations on their electronic configurations. For instance, the metal–metal overlap population computed with the EH method is rather strong (0.11) in the electron-poor cluster **13**. This reflects again the rather nonbonding or weak antibonding nature of the top of the d band in these cubic compounds. Except for the inversion order between the close HOMO and LUMO ($1a_{2u}$ and $2e_u$), the EH and Xα MO diagrams are similar. According to our Xα calculations, the singly occupied $1a_{2u}$ HOMO is found to be almost degenerate with the $2e_u$ LUMO (the computed HOMO–LUMO gap is 0.02 eV). The other vacant d levels are $2t_{1u}$, $2e_g$, $3t_{2g}$, $2t_{1g}$, and $3t_{1u}$, as expected (see Figure 2 for the labeling). Note that our Xα calculations found the $(1a_{2u})^1(2e_u)^0$ ground-state configuration 0.09 eV more stable than the $(1a_{2u})^0(2e_u)^1$ one.

With one more electron, Xα calculations find the $(1a_{2u})^2(2e_u)^0$ ground-state configuration to be slightly preferred over the $(1a_{2u})^1(2e_u)^1$ and $(1a_{2u})^0(2e_u)^2$ ones by 0.11 and 0.18 eV, respectively. The energy gap between the $1a_{2u}$ and $2e_u$ MOs is ca. 0.02 eV. Therefore, whatever is the actual occupation of the $(1a_{2u} + 2e_u)$ set, Jahn–Teller instability is expected, leading to some symmetry lowering. Indeed, the symmetry observed in compound **12** for instance is either C_i or C_{4h} depending on the counterion.[10] However, the distortion away from O_h is weak, in agreement with the weak metal–metal antibonding nature of the involved levels (see, for example, Figure 3).

Fewer Terminal Ligands: The Electronic Structure of the Terminal Ligand-Deficient $M_8(\mu_4\text{-}E)_6L_n$ Species

Five compounds listed in Table 1 (**15–19**) possess an incomplete surrounding shell of terminal ligands. Surprisingly, they all bear an MVE count smaller than 120. Indeed, for a given structure, the electron count of a mono- or polynuclear transition-metal complex is expected to remain unchanged when a 2-electron ligand is removed. In other words, the bonding M–L electron pair which is lost is generally replaced by a nonbonding pair localized on the metal center in order to maintain the stability of the complex. The two MOs (σ and σ^*) associated with an M–L bond of an N-electron M_xL_y species are represented on the top of Figure 5a. They can be described as the bonding (occupied) and antibonding (vacant) combinations of the σ FMO of L with a metallic FMO predominantly d in character. The MOs of the dissociated system, M_xL_{y-1} + L, are shown on the bottom of the same figure. The two FMOs do not interact anymore (they do not overlap). They become nonbonding and lie at relatively low energy. Specifically, the metallic σ FMO joins the metallic d block. The M_xL_{y-1} species will be stable if its low-lying orbitals are occupied and if the HOMO–LUMO gap is large. Consequently, the metallic σ FMO close to the metallic d block should be populated, leading to a count of N electrons as in the M_xL_y complex.

The situation is different if, instead of a metallic d FMO, an sp hybrid is used for the σ_{M-L} bond (see Figure 5b). Indeed, the nonbonding metallic FMO released upon removal of the ligand remains high in energy, being mainly s and p in character, and therefore unoccupied. Consequently, the total electron count of the M_xL_{y-1} species decreases by 2 units compared to that of the M_xL_y one. This type of electron deficiency is somewhat related to that of square-planar ML_4 species, which are usually characterized by 16 instead of 18 electrons, due to the high energy of one metallic nonbonding p level.[23]

In the $Ni_8(\mu_4\text{-}E)_6L_8$ species, each metal center which is surrounded by a tetrahedron of ligands utilizes an sp hybrid to bind with its terminal phosphine ligand (the other orbitals either are used for Ni–Ni or Ni–P bonding or are not symmetry-adapted). The loss of one (or several) L ligand(s) generates one (or several) nonbonding sp MO(s) on one (or several) Ni center(s), which lie(s) at rather high energy and must remain vacant. This is illustrated in Figure 6, which represents the MO diagrams of the various isomers of the models $Ni_8(\mu_4\text{-}PH)_6(PH_3)_{8-n}$ ($0 \leq n \leq 8$) calculated with the EH method. As one can see, when a terminal ligand is pulled out, a high-lying nonbonding metallic level appears, and the favored electron count (corresponding to a large HOMO–LUMO gap, see Figure 6) diminishes by 2 units.

(26) (a) Kim, J.; Rees, D. C. *Science* **1992**, *257*, 1677; (b) *Nature* **1992**, *360*, 553.

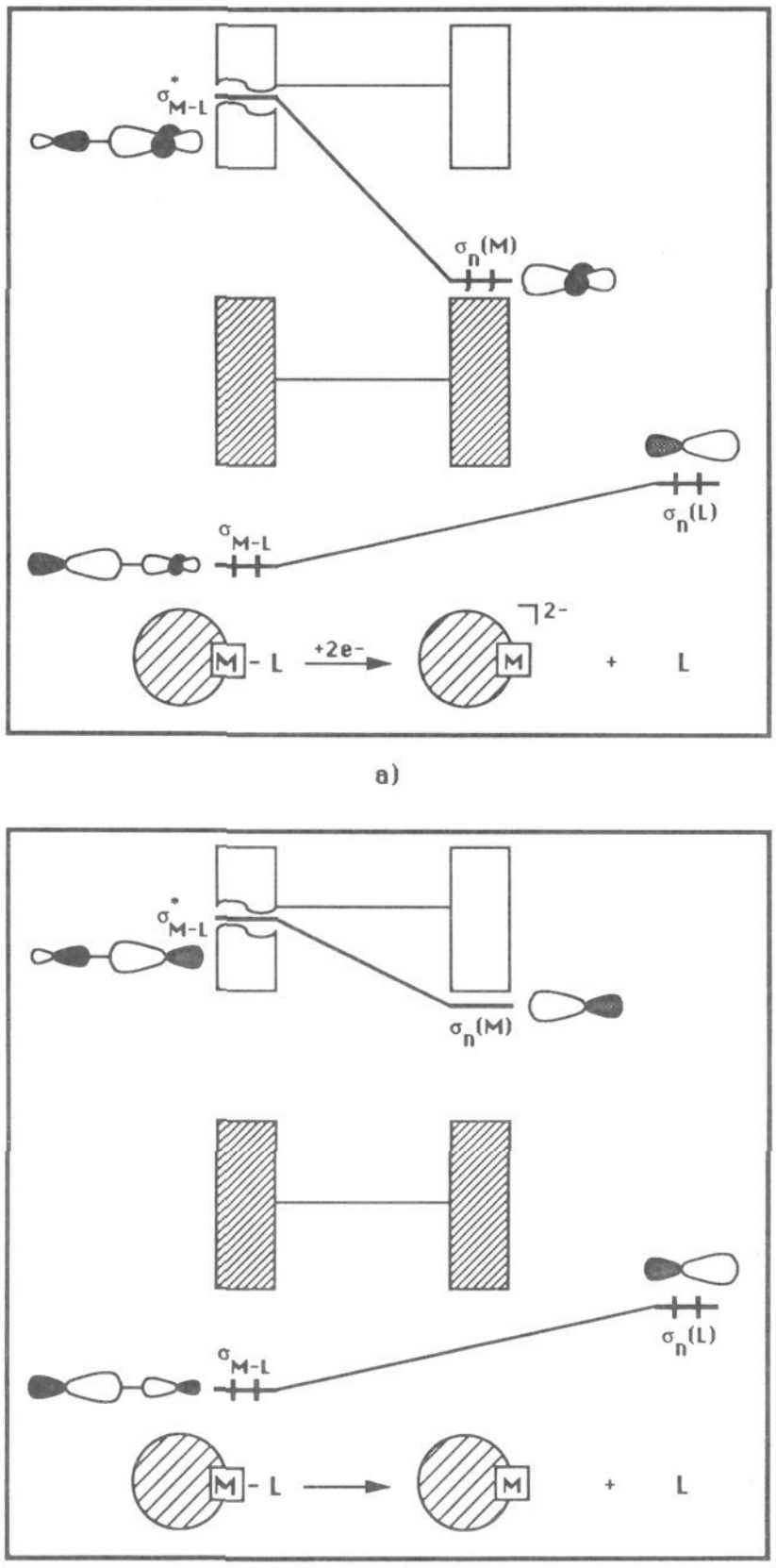

Figure 5. Electronic effect of the loss of a terminal ligand in an M_xL_y cluster species: (a) usual case where the M–L bond is ensured by a d-type metallic orbital; (b) peculiar case where the M–L bond is ensured by an sp-type metallic orbital.

As a consequence, the favored MVE count of the $M_8(\mu_4\text{-}E)_6L_n$ compounds is equal to $120 - 2(8 - n)$. For instance, an MVE count of 104 is expected for the cubic species $Ni_8(\mu_4\text{-}PH)_6$ having no terminal ligands ($n = 0$). This peculiar electron count was also found by Rösch and co-workers using LCGTO-LDF calculations.[22] The large HOMO–LUMO gaps computed for all the models are consistent with a diamagnetic behavior. This is in disagreement with some experimental data, which suggest that the 114- and 112-electron species, **16** and **19**, respectively, are paramagnetic.[8] In order to check the EH results, Xα calculations have been performed on $Ni_8(\mu_4\text{-}PH)_6(PH_3)_4$ of symmetry T_d, used to model species **19**. They lead to the same results, i.e., the same ground-state closed-shell electronic configuration with a large HOMO–LUMO gap (1.65 and 1.03 eV with the EH and Xα methods, respectively) for the count of 112 electrons. For compound **16**, one could think that the paramagnetic behavior is due to the terminal Ni atom borne by one of the Ni centers. In fact, EH calculations carried out on the model $Ni_8(\mu_4\text{-}PH)_6(PH_3)_4Ni$ show comparable results to that of

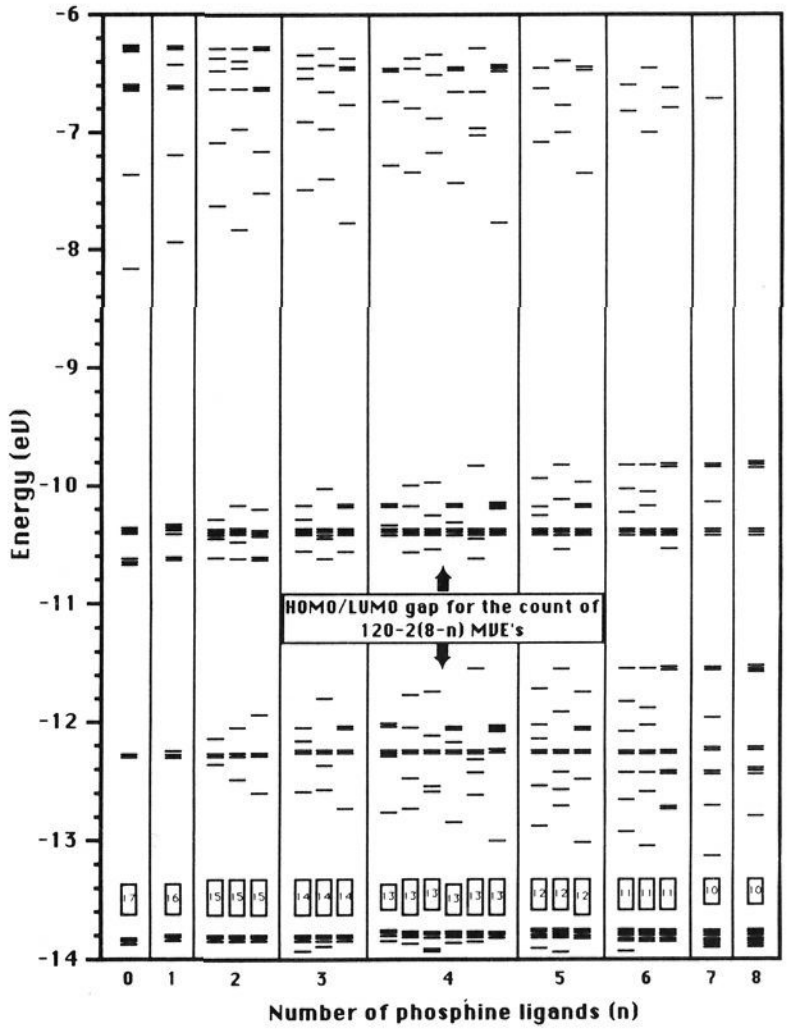

Figure 6. EH MO diagrams for the models $Ni_8(\mu_4\text{-}PH)_6(PH_3)_n$ with n varying from 0 to 8. For $n = 2$, 3, 4, 5, and 6, and MO diagrams of the different geometrical isomers are given.

the isoelectronic species $Ni_8(\mu_4\text{-}PH)_6(PH_3)_5$. The "bare" d^{10} Ni atom plays the role of a 2-electron ligand using a $z^2/s/z$ hybrid orbital to bind with one of the Ni atoms of the cube. Its nonbonding d orbitals are low in energy and occupied, while the s orbital is destabilized and constitutes the cluster LUMO. A large HOMO–LUMO gap of 1.44 eV is observed, suggesting here again a closed-shell electronic configuration. Clearly, more accurate experimental measurements on those species would be needed in order to confirm or not confirm our results.

The coordination deficiency of some Ni centers in the $M_8(\mu_4\text{-}E)_6L_n$ species leads to a weak distortion of the metallic cube. Additional Ni–Ni bonding occurs between nonadjacent Ni atoms to which no terminal ligand is attached. For instance, contraction of the cube along a solid diagonal and along face diagonals is observed in compounds **15** and **18**, respectively.[5] The origin of this attractive interaction between nonbonded metals is due to second-order mixing of an in-phase combination of the free sp Ni hybrids into occupied levels of proper symmetry.

Finally, it should be noted that, as for the 120 MVE count in the $M_8(\mu_4\text{-}E)_6L_8$ species, the count of $[120 - 2(8 - n)]$ electrons must be considered as the maximum value for $M_8(\mu_4\text{-}E)_6L_n$ compounds. This optimal number is expected for clusters made of electronegative metal atoms bearing ligands such as carbonyls or phosphines. With less electronegative metal atoms (Co, Fe, ...) and π-donor ligands, species with lower electron counts might exist.

Other Metallic M_8 Clusters Bearing π-Donor Ligands

Some years ago, Fackler, Coucouvanis, and co-workers characterized copper cubic cluster salts such as $[(NPhMe_3)_4Cu_8(i\text{-}MNT)_6]$ (i-MNT = $S_2CC(CN)_2$),[27] $[(PPh_4)_4Cu_8(DTS)_6]$ (DTS = $S_2C_4O_2$),[28] and $[(PPh_4)_4Cu_8(DED)_6]$ (DED = $S_2CC(COEt)_2$).[29]

(27) McCandlish, L. E.; Bissell, E. C.; Coucouvanis, D.; Fackler, J. P.; Knox, K. *J. Am. Chem. Soc.* **1968**, *90*, 7357.
(28) Hollander, F. J.; Coucouvanis, D. *J. Am. Chem. Soc.* **1974**, *96*, 5646.
(29) Hollander, F. J.; Caffery, M. L.; Coucouvanis, D. *Abstracts on Papers*, 167th National Meeting of the American Chemical Society, Los Angeles, CA, March 31–April 5, 1974; American Chemical Society: Washington, DC, 1974; INOR 73.

Such compounds, which exhibit a cubic $[Cu_8(\mu\text{-}S)_{12}]^{4-}$ core of T_h symmetry with the S atoms of the bidendate ligands bridging the edges of the cube, are characterized by a count of 128 MVEs, i.e., $16n$, if n represents the number of Cu centers. Assuming a formal charge of 2- per chelate ligand, each Cu atoms has a formal oxidation state of 1+. A Cu–Cu bond order of $^2/_3$ is then necessary in order to satisfy the 18-electron rule around each Cu atom. Surprisingly, previous calculations suggest no net bonding between the copper atoms.[30] Let us mention that a cubic $Cu_8(\mu\text{-}E)_{12}$ core of T_h symmetry has been recently reported in the solid-state material $K_4Cu_8Te_{11}$.[31] The formal oxidation state of Cu in the cubic $Cu_8(Te_2)_6$ entities is also 1+, and the Cu–Cu separations (ca. 2.8 Å) are comparable to that measured in the molecular Cu species mentioned above.

The recent discovery of the molecular metallocarbohedrene clusters like $Ti_8(C_2)_6$ or $V_8(C_2)_6$ must be mentioned here since a dodecahedral M_8E_{12} arrangement of T_h symmetry, analogous to the one encountered in $K_4Cu_8Te_{11}$, has been proposed.[32] Recent theoretical studies have shown the stability of such architectures for a small count of 44 MVEs.[33]

There are other ways to assemble eight metallic atoms.[7] The compound $Co_8(\mu_4\text{-}Se)_2(\mu_3\text{-}Se)_6(PPh_3)_6$ provides an example in which the metallic edifice consists of two square pyramids sharing an edge.[34] Application of the condensation electron-counting rules leads to a count of 74(2) – 34 = 114 electrons, where 74 is the usual count for a square-pyramidal M_5 cluster and 34 the count characteristic of the common edge.[35] The observed count is 116 electrons. A theoretical study is in progress in our laboratory to rationalize this kind of condensed electron-rich species.

Conclusions

The molecular orbital studies described in this paper on $M_8(\mu_4\text{-}E)_6L_n$ cluster compounds have indicated that their optimal number of MVEs is 120. This count is favored with terminal π-acceptor ligands. The rather strong M–M bonding is mainly due to through-space M–M bonding interactions but also to through-bond interactions via metal-to-capping ligand bonding. A delocalized bonding picture is therefore necessary to describe their electronic structure. For such an electron count, the M-(μ_4-E) bonding is maximized, whereas the M–M bonding is not. The latter is strengthened upon depopulation of the top of the d band. Open-shell electronic configurations are then expected, as observed for clusters bearing terminal π-donor ligands. The slight antibonding/nonbonding nature of the top of the metallic d band allows a large range of electron counts (from 99 to 120, so far) without altering the cubic metallic core. Smaller electron counts with early transition metals might be possible, the lowest theoretical limit being 76 MVEs.

When terminal ligands borne by the metal atoms are missing, the expected count for compounds of formula $M_8(\mu_4\text{-}E)_6L_n$ is 120 – 2(8 – n) MVEs. In cubic $M_8(\mu_4\text{-}E)_6L_n$ species, M–L bonds result from the combination between a metallic sp hybrid and the σ lone pair orbital of L. When n terminal ligands are lost, the corresponding metallic sp hybrids become nonbonding but remain high in energy and cannot be occupied, leading to an electron count diminished by $2n$ units compared to that of the $M_8(\mu_4\text{-}E)_6L_8$ parent species. This electron count occurring for electronegative metal atoms and terminal π-acceptor ligands might decrease with less electronegative metal atoms and/or termiinal π-donor ligands.

Finally, let us mention that in some cases, an additional metal atom can be "swallowed" in the center of the metallic core of cubic clusters, leading to more electron-rich compounds of the formula $M_9(\mu_4\text{-}E)_6L_8$, such as $Ni_9(\mu_4\text{-}GeEt)_6(CO)_8$.[36] The electronic structure of this peculiar family of centered metallic cubic species will be described in a subsequent paper.[37]

Acknowledgment. We are grateful to Dr. R. L. Johnston for helpful comments and Prof. D. Fenske for provision of some structural data.

Appendix

(a) Extended Hückel Calculations. Calculations have been carried out within the extended Hückel formalism[38] using the weighted H_{ij} formula.[39] The standard atomic parameters utilized were taken from literature. The different models used were based on the idealized experimental molecular compounds.[1-11] The following bond distances (Å) were used: Ni–Ni = 2.60; Ni–(μ_4-P) = 2.21; Ni–P(H_3) = 2.25; Ni–C(O) = 1.78; Ni–Cl = 2.25; P–H = 1.42; C–O = 1.14 in the Ni species; Co–Co = 2.67; Co–(μ_4-S) = 2.24; Co–S = 2.28; S–H = 1.30 in the Co species; Fe–Fe = 2.72; Fe–(μ_4-S) = 2.32; Fe–I = 2.50 in $[Fe_8(\mu_4\text{-}S)_6I_8]^{3-}$.

(b) SCF-MS-Xα Calculations. The standard version of the density functional SCF-MS-Xα method[40] was used and applied to models $Ni_8(\mu_4\text{-}PH)_6(CO)_8$, $Ni_8(\mu_4\text{-}PH)_6(PH_3)_4$, and $[Fe_8(\mu_4\text{-}S)_6I_8]^{4-/3-}$ of O_h, T_d, and O_h symmetry, respectively. The considered molecular geometries used were the same as those used for the EH calculations.[1-11] The calculations on $[Fe_8(\mu_4\text{-}S)_6I_8]^{4-}$ were simply performed by adding one electron to the electronic spectrum of $[Fe_8(\mu_4\text{-}S)_6I_8]^{3-}$. The atomic radii of the muffin-tin spheres r (Å) and the exchange scaling parameters α, taken from the tabulation of Schwarz[41] for heavy elements and from an article from Slater[42] for the H. A Watson sphere[43] having the same radius as the outer sphere and bearing the 3+ and 4+ charges have been introduced in the calculations of $[Fe_8(\mu_4\text{-}S)_6I_8]^{3-}$ and $[Fe_8(\mu_4\text{-}S)_6I_8]^{4-}$, respectively, in order to mimic the external stabilizing electrostatic field. The maximum l values in the partial wave expansion included in the calculations were l = 2 for Ni, Fe, I, S, and outer spheres, l = 1 for P, O, and C spheres, and l = 0 for H sphere.

Supplementary Material Available: Tables of one-electron energies and charge distributions for $Ni_8(\mu_4\text{-}PH)_6(CO)_8$, $Ni_8(\mu_4\text{-}PH)_6(PH_3)_3$, and $[Fe_8(\mu_4\text{-}S)_6I_8]^{3-}$, obtained from X$\alpha$ calculations; tables of EH and SCF-MS-Xα parameters; Xα MO diagram of the d block in the 99-electron compound $[Fe_8(\mu_4\text{-}S)_6I_8]^{3-}$ (6 pages). This material is contained in many libraries on microfiche, immediately follows this article in the microfilm version of the journal, and can be ordered from the ACS; see any current masthead page for ordering information.

(30) Avdeef, A.; Fackler, J. P. *Inorg. Chem.* **1978**, *17*, 2182.
(31) Park, Y.; Kanatzidis, M. G. *Chem. Mater.* **1991**, *3*, 781.
(32) (a) Guo, B. C.; Kerns, K. P.; Castleman, A. W., Jr. *Science* **1992**, *255*, 1411. (b) Guo, B. C.; Wei, S.; Purnell, J.; Buzza, S.; Castleman, A. W. Jr. *Science* **1992**, *256*, 515. (c) Wei, S.; Guo, B. C.; Purnell, J.; Buzza, S.; Castleman, A. W., Jr. *Science* **1992**, *256*, 818; (d) *J. Chem. Phys.* **1992**, *96*, 4166. (e) Cartier, S. F.; Chen, Z. Y.; Walder, G. J.; Sleppy, C. R.; Castleman, A. W., Jr. *Science* **1993**, *260*, 195.
(33) (a) Grimes, W.; Gale, J. D. *J. Chem. Soc., Chem. Commun.* **1992**, 1222. (b) Dance, I. *J. Chem. Soc., Chem. Commun.* **1992**, 1779. (c) Rohmer, M. M.; de Vaal, P.; Bénard, M. *J. Am. Chem. Soc.* **1992**, *114*, 9696. (d) Lin, Z.; Hall, M. B. *J. Am. Chem. Soc.* **1992**, *114*, 10054. (e) Reddy, B. V.; Khanna, S. N.; Jena, P. *Science* **1992**, *258*, 1640. (f) Methfessel, M.; van Schiefgaarde, M.; Scheffer, M. *Phys. Rev. Lett.* **1992**, *70*, 29. (g) Ceulemans, A.; Fowler, P. W. *J. Chem. Soc., Faraday Trans.* **1992**, *88*, 2797. (h) Pauling, L. *Proc. Natl. Acad. Sci. U.S.A.* **1992**, *89*, 8175.
(34) Fenske, D.; Ohmer, J.; Merzweiler, K. *Z. Naturforsch.* **1987**, *42b*, 803.
(35) Mingos, D. M. P. *J. Chem. Soc., Chem. Commun.* **1983**, 706.
(36) Zebrowski, J. P.; Hayashi, R. K.; Bjarnason, A.; Dahl, L. F. *J. Am. Chem. Soc.* **1992**, *114*, 3121.
(37) Furet, E.; Le Beuze, A.; Halet, J.-F.; Saillard, J.-Y., to be submitted (part 2 in this series).
(38) (a) Hoffmann, R. *J. Chem. Phys.* **1963**, *39*, 1397. (b) Hoffmann, R.; Lipscomb, W. N. *J. Chem. Phys.* **1962**, *36*, 2179.
(39) Ammeter, J. H.; Bürgi, H.-B.; Thibeault, J. C.; Hoffmann, R. *J. Am. Chem. Soc.* **1978**, *100*, 3686.
(40) Johnson, K. H. *Adv. Quantum Chem.* **1973**, *7*, 143.
(41) (a) Schwarz, K. *Phys. Rev. B* **1972**, *5*, 2466. (b) Schwarz, K. *Theoret. Chim. Acta* **1974**, *34*, 225.
(42) Slater, J. C. *Int. J. Quantum Chem.* **1973**, *7*, 533.
(43) Watson, R. E. *Phys. Rev.* **1958**, *111*, 1108.